

Linking Observations of the Asian Monsoon to the Indian Ocean SST: Possible Roles of Indian Ocean Basin Mode and Dipole Mode

JIANLING YANG

Physical Oceanography Laboratory, and Ocean–Atmosphere Interaction and Climate Laboratory, Ocean University of China, Qingdao, and Key Laboratory of Meteorological Disaster Preventing and Reducing in Ningxia, Ningxia Climate Center, Yinchuan, China

QINYU LIU

Physical Oceanography Laboratory, and Ocean–Atmosphere Interaction and Climate Laboratory, Ocean University of China, Qingdao, China

ZHENGYU LIU

Physical Oceanography Laboratory, and Ocean–Atmosphere Interaction and Climate Laboratory, Ocean University of China, Qingdao, China, and Center for Climatic Research, University of Wisconsin—Madison, Madison, Wisconsin

(Manuscript received 8 December 2008, in final form 11 January 2010)

ABSTRACT

The authors investigate the relationship between sea surface temperature (SST) in the tropical Indian Ocean (TIO) and the seasonal atmosphere circulation in the Asian monsoon region (AMR) using the maximum covariance analyses (MCAs). The results show that the Asian monsoon circulation is significantly correlated with two dominant SST anomaly (SSTA) modes: the Indian Ocean Basin mode (IOB) and the Indian Ocean dipole mode (IOD). The peak SSTA of the IOB appears in spring and has a much stronger relationship with the Asian summer monsoon than the peak of the IOD does, whereas the peak SSTA for the IOD appears in fall and shows a stronger link to the Asian winter monsoon than to the Asian summer monsoon. In addition, the IOB in spring has a relatively stronger link with the atmospheric circulation in summer than in other seasons.

The large-scale atmospheric circulation and SSTA patterns of the covariability of the first two dominant MCA modes are described. For the first MCA mode, a warm IOB, persists from spring to summer, and the atmospheric circulation is enhanced by the establishment of the climatological summer monsoon. The increased evaporative moisture associated with the warm IOB is transported to South Asia by the climatological summer monsoon, which increases the moisture convergence toward this region, leading to a significant increase in summer monsoon precipitation. For the second MCA mode, a positive IOD possibly corresponds to a weaker Indian winter monsoon and more precipitation over the southwestern and eastern equatorial TIO.

1. Introduction

Sea surface temperature (SST) in the tropical Indian Ocean (TIO) varies significantly at interannual time scales. This variability is dominated by an Indian Ocean Basin mode (IOB) and Indian Ocean dipole mode (IOD).

The IOB is the first empirical orthogonal function (EOF) mode of the SST anomaly (SSTA), accounting for about 30% of the total variance of the TIO SSTA. The IOD is the second EOF mode of the SSTA, accounting for about 12% of the total variance of the TIO SSTA (Saji et al. 1999; Webster et al. 1999).

The potential roles of the Indian Ocean SSTA in the Asian summer monsoon have been sought as predictive information on the monsoon (e.g., Zhu 1993; Zhu and Houghton 1996; Clark et al. 2000; Yoo et al. 2006; Izumo et al. 2008; Wu et al. 2008). It has been found that the SSTA over the Arabian Sea and the southern Indian

Corresponding author address: Qinyu Liu, Physical Oceanography Laboratory and Ocean–Atmosphere Interaction and Climate Laboratory, Ocean University of China, 238 Songling Road, Qingdao 266100, China.
E-mail: liuqy@ouc.edu.cn

Ocean can play a significant role in the Asian monsoon. The studies of the tropospheric biennial oscillation have shown strong interannual relationship between the TIO SSTA and the Indian monsoon on a biennial time scale (Meehl 1997; Meehl and Arblaster 2002; Meehl et al. 2003). A warming in the TIO enhances the Indian summer monsoon, which leads to a strong Australian monsoon in the subsequent boreal winter. Generally, however, it was found that the TIO SST–monsoon relationship is complex and always associated with El Niño–Southern Oscillation (ENSO).

About 10 years ago, the roles of the Indian Ocean SSTA in the Asian monsoon started to receive renewed attention, largely because of the studies of the IOD and its potential effect on the Asian monsoon (Saji et al. 1999; Webster et al. 1999). Most studies have shown that the IOD correlates significantly with the Asian summer monsoon (Behera et al. 1999; Slingo and Annamalai 2000; Ashok et al. 2001; Li and Mu 2001; Behera and Yamagata 2003; Guan et al. 2003; Li et al. 2003; Saji and Yamagata 2003; Lau and Nath 2004; Kripalani et al. 2005; S. Yang et al. 2007; Yuan et al. 2008a). These studies show the IOD not only correlates with the Asian monsoon around the TIO rim but also with climate variability over remote areas, such as East Asia, Europe, and even America. Most previous studies focused on the roles of the IOD in summer monsoon, although some authors investigated the IOD relationship with South Asia rainfall in late fall (Kripalani and Kumar 2004) and Sri Lanka rainfall in fall (Lareef et al. 2003). The IOD peaks in fall; its relation with the atmosphere in seasons other than summer has not been studied extensively. In addition, a recent study (Kulkarni et al. 2007) showed the summer monsoon rainfall over South Asia has more influence on the IOD in fall than the other way around. Therefore, it is necessary to reexamine the relationship between the IOD and atmosphere circulation in Asia.

In contrast, relatively less attention has been paid to the IOB and its roles in the Asian monsoon until the last several years. Perhaps because the IOB is well known to be related closely to the Pacific ENSO and therefore its roles in monsoon are also associated with ENSO. Some studies have investigated the atmospheric response to the ENSO-induced SSTA in the Indian Ocean/western Pacific Ocean by observations and model simulations (Lau and Nath 2000, 2003; Loschnigg et al. 2003; Kumar and Hoerling 2003; Watanabe and Jin 2003; Alexander et al. 2004; Lau et al. 2004, 2005; Shinoda et al. 2004; Terray et al. 2005; Izumo et al. 2008; Xie et al. 2009; Park et al. 2009). The atmosphere response to the SSTA in the Indian Ocean/western Pacific is dominated by a pair of geopotential height anomalies that are symmetric about the equator and centered over the extratropics in boreal

summer after the mature phase of ENSO (Kumar and Hoerling 2003; Lau et al. 2005). Wang et al. (2000) showed that the delayed effect of ENSO on the East Asian summer monsoon is through the Philippine Sea anticyclone. Using a simple linear model forced by the TIO SSTA during the boreal winter of El Niño years, Watanabe and Jin (2003) noted that an increase in precipitation over the western TIO is accompanied by a decrease in precipitation over the tropical western Pacific–Maritime Continent, and they argued that this suppressed precipitation strengthens the Philippine Sea anticyclone. Lau and Nath (2000, 2003) and Lau et al. (2004) used general circulation model (GCM) experiments to demonstrate that the SSTA induced by the atmospheric bridge mechanism could in turn feed back to the atmospheric circulation and lead to an increase in the summer monsoon rainfall over South Asia in the following year of El Niño events.

Recently, there have been some studies on the roles of the IOB in the Asian monsoon region (AMR) atmosphere. In an atmospheric GCM, Annamalai et al. (2005a) examined monsoon responses to the IOB during winter and spring after the mature phase of El Niño. In an observational and coupled model analysis, J. Yang et al. (2007) studied the IOB influences on the AMR atmosphere into summer, identifying the role of the IOB in prolonging the influence of ENSO on the Asian summer monsoon. Li et al. (2008) and Yuan et al. (2008b) further explored the roles of the IOB SSTA in different components of the Asian monsoon.

In short, the TIO SSTA is often believed to play an important role in the Asian monsoon. However, there are two dominant modes of the SSTA in the TIO: IOB and IOD. Which mode plays a more important role in the Asian monsoon and in which season? What are the physical mechanisms behind the effects of the IOB or the IOD? The purposes of this study are twofold. First, we estimate together the effects of the IOB and the IOD and show the relative importance of those two modes in a consistent way by means of maximum covariance analysis (MCA) (Czaja and Frankignoul 2002). A general picture of the TIO SSTA linkage to the atmosphere over the AMR is given. Second, we further describe the large-scale patterns of the covariability of the first two dominant MCA modes.

The paper is organized as follows. In section 2 the data and methods are described. On the basis of the MCA results, the first two coupled modes of the SSTA in the TIO and atmosphere circulation anomaly in the AMR are given in section 3. In sections 4 and 5, the large-scale patterns of the covariability about the first two MCA-dominant modes are described. Discussion and conclusions of this study follow in section 6.

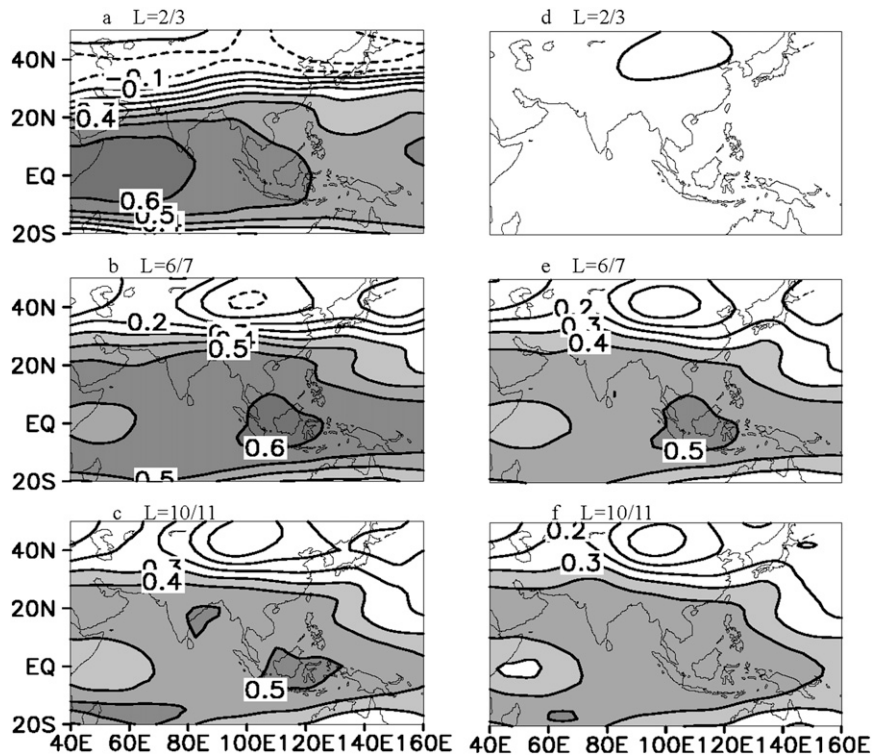


FIG. 1. (left) The 2-month mean of the correlations coefficient between the H200A in JJA and the Niño-3 index of the (a) preceding AMJ and MAM, (b) preceding DJF and NDJ, and (c) preceding ASO and JAS. (right) As in (left), but for the H200A without the ENSO effect signal that was removed using a linear regression of the Niño-3 index of 2 months prior.

2. Data and filtering of the ENSO effect

The National Centers for Environmental Prediction–National Center for Atmospheric Research (NCEP–NCAR) reanalysis (Kalnay et al. 1996) is used to derive the monthly data of the geopotential height at 200 hPa (hereafter H200), horizontal wind and specific humidity at 850 hPa, vertical velocity (ω) at 500 hPa, precipitation rate, and vertically integrated atmosphere heat source in the AMR, defined here as the area of 20°S–50°N, 40°–160°E. The vertically integrated atmosphere heat source is calculated using the method proposed by Yanai and Tomita (1998). The monthly SST data come from the Hadley Centre Global Sea Ice and Sea Surface Temperature (HadISST) dataset over the TIO region (20°S–20°N, 40°–110°E). The Niño-3 index is defined, as usual, as the SST averaged in the eastern equatorial Pacific over 5°S–5°N, 90°–150°W. All data are in the period 1950–2004, except for the atmosphere heat source that is for 1958–2000.

This direct effect of ENSO on the atmosphere can be shown clearly in the 2-month mean of correlation between the June–August (JJA) H200 and the Niño-3 SST of preceding months (Fig. 1). As the Niño-3 SST leads

the H200 by 0–3 months, the high H200 correlation occupies the entire equatorial belt. These correlation patterns are consistent with earlier studies of the direct ENSO effect on the atmospheric circulation (Chiang and Sobel 2002; Kumar and Hoerling 2003; Lau et al. 2005). As pointed out by these previous studies, the response of H200 is the equatorial Kelvin wave response that extends eastward from the heat source region over the eastern equatorial Pacific into the Indian Ocean. When ENSO leads further by 4–5 months up to 10–11 months (only showing at lag = 6–7 and 10–11 in Figs. 1b,c), high correlations are found in the subtropics on either side of the equator west of 80°E while it is trapped on the equator to the east over the Maritime Continent, reminiscent of the atmosphere Rossby wave and Kelvin wave responses to a tropical heating centered on the TIO (Gill 1980). Along the equator, H200 anomaly correlation with Niño-3 index reaches a meridional maximum east of 90°E but a meridional minimum to the west, an east–west asymmetry caused by the eastward propagation of the Kelvin wave forced by a zonally confined heat source over the TIO.

The direct effect of ENSO can be removed from the atmospheric data with a linear regression of the Niño-3

SST anomaly (2 months earlier) at each grid point. Now, the JJA H200 anomaly (H200A) is no longer correlated with the Niño-3 SSTA, as the Niño-3 SSTA leads by 0–3 months (for concision, Fig. 1d only shows at lag = 2–3). However, as the Niño-3 SSTA leads by more than 4 months, the correlation coefficient (only showing at lags 6–7 and 10–11 in Figs. 1e,f) shows a Matsuno–Gill response pattern that is very similar to the response before the removal of the ENSO effect (Figs. 1b,c), albeit with a correlation value somewhat reduced. The correlation peaks at the lead of 8–11 months, implying a significant correlation to the peak month of the Niño-3 SSTA in the preceding winter (Fig. 1f). This much-delayed atmospheric response to ENSO is consistent with the capacitor response of the TIO SSTA to ENSO (J. Yang et al. 2007).

In addition, we have examined other techniques for removing ENSO, that is using Niño-3.4 and the first three principal components of the EOFs of SSTs in the tropical Pacific to construct an ENSO index (Park et al. 2006). The results are almost the same as those using the Niño-3 index. It is worth noting that we only remove the linear direct signal, not all signals of ENSO, from the atmospheric data.

3. MCA

a. Method

To investigate the interaction between the atmosphere over the AMR and the TIO SSTA, the MCA is applied to the fields of the TIO SSTA and the AMR H200 anomaly (H200A) following the procedure of Czaja and Frankignoul (2002). The MCA method applies the singular value decomposition (SVD) to a pair of geophysical fields (Bretherton et al. 1992) at different lead/lag and has been shown successfully in shedding light on the interaction between the atmosphere and SSTA in the Atlantic (Czaja and Frankignoul 2002) and Pacific Oceans (Q. Liu et al. 2006; Frankignoul and Sennechael 2007).

Following Czaja and Frankignoul (2002), homogeneous maps for SSTA and atmospheric variables are scaled to represent the amplitude of SSTA and atmospheric variables associated with one standard deviation of MCA time series of SSTA. For each lag, the statistical significance of the squared covariance (SC) and the SC fraction (SCF) between time series of SSTA and H200A is tested with a Monte Carlo approach, randomly permuting the years—but not the months—of the SSTA sequence. The quoted significance levels indicate the percentage of randomized SC and SCF for the corresponding modes that exceed the value being tested.

Before the MCA analysis, monthly anomalies are constructed by removing mean seasonal cycles. A third-order polynomial is then generated by least squares fit of the

anomaly time series, removing the trends and low frequencies displayed in the analysis period. These monthly anomalies are weighted by the square root of the cosine of latitude to ensure proper area weighting in the analysis. To give similar weight to each month, hence increasing the effective number of degrees of freedom, monthly anomalies are normalized by a mean (domain averaged) seasonal cycle of standard deviation, and the covariance matrixes between SSTA and H200A are estimated, with monthly anomalies binned into groups of three months (i.e., the length N of the time series is usually $N = 3 \times 55$ yr) and then the SVD method is used to decompose the covariance matrixes.

b. MCA results

We first perform the MCA between the SSTA in the TIO (20°S–20°N, 40°–110°E) and the full H200A in the AMR (20°S–50°N, 40°–160°E), with the full ranges of signals including ENSO. Figures 2a–d show the SCs and SCFs of the first two MCA modes, with the SCs and SCFs plotted as a function of calendar month of H200A (x axis) and lead–lags (y axis). A negative lag corresponds to the SSTA leading the H200A. The SC of the first MCA mode is significant at the 99% confidence level (shading) in almost all seasons and for all the lags. However, this mode should be dominated by the direct ENSO effect, because the SC peaks during winter when ENSO peaks, with a nearly in-phase relationship between the H200A and the SSTA. Furthermore, the SC pattern shows a largely symmetric structure, with the SCF between 90%–95%. As such, the covariance between the H200A and the SSTA is significantly contributed to by the autocorrelation of the long persistent ENSO itself. This largely symmetric SC with lags differs dramatically from those in the extratropical ocean–atmosphere system over the North Atlantic (Czaja and Frankignoul 2002), where the SC is strongly asymmetric with lags, with the SC peaking as the SSTA lags the atmosphere by 1 month, reflecting the dominant local atmospheric forcing on the SSTA.

The SCF of the second MCA mode is less than 20%, and there are fewer areas with significance over the 99% confidence level in Figs. 2c,d. In addition, the second mode peaks in fall [August–October (ASO) to October–December (OND)] for the H200A with the SSTA leading by 1 month (lag = -1). As will be discussed later, this mode represents the role of the IOD (Saji et al. 1999; Webster et al. 1999) in the atmospheric circulation over the AMR.

To isolate the TIO linkage to the atmosphere, we need to filter out the direct ENSO signal. As discussed in section 2, the direct ENSO effect is filtered from the atmospheric field at each grid point with a linear regression

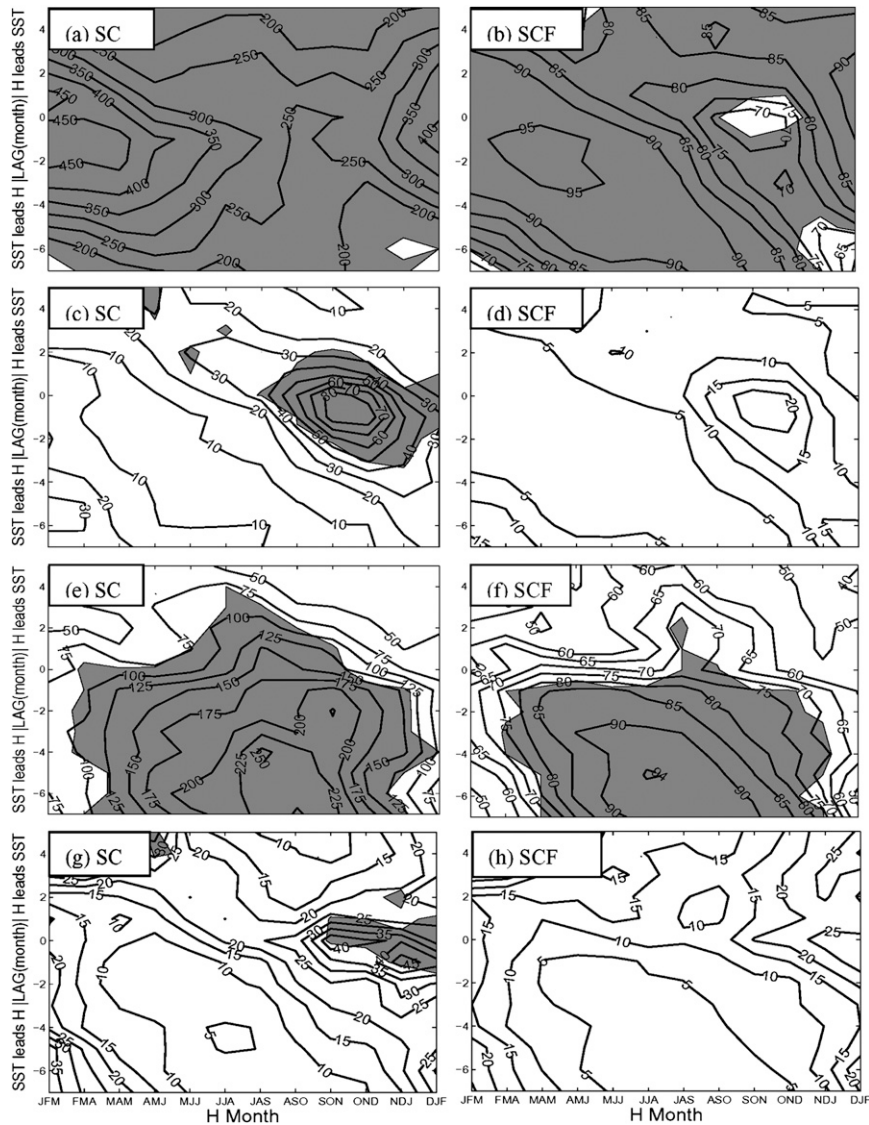


FIG. 2. The (left) SC and (right) SCF of the (a),(b),(e),(f) first MCA mode and (c),(d),(g),(h) second MCA mode between the TIO SSTA and the AMR H200A (a)–(d) with and (e)–(h) without the ENSO effect. Shading indicates $>99\%$ significance. The abscissa is the AMR H200A the calendar month, while the ordinate is lag, positive (negative) for AMR H200A leading (lagging) TIO SSTA.

of the Niño-3 SST index. The subsequent MCA between the TIO SSTA and the AMR H200A shows the first MCA mode (Figs. 2e,f) with the SC–SCFs structure differing significantly from that before the filtering (Figs. 2a,b). First of all, the statistical significance is greatly reduced, with the large parameter regime at the 99% insignificance level. Most importantly, the SCs–SCFs now peak in the summer monsoon season and the TIO SSTA leads by around one season, with the corresponding SCF reaching more than 90%. This shows, after removing the direct ENSO signal from the atmospheric, that peak

summer monsoon circulation is correlated predominantly with the TIO SSTA in the preceding spring. This TIO SSTA role reflects the dominant linkage of the IOB to the Asian summer monsoon and will be discussed further in section 4.

It is interesting to compare the TIO linkage to the atmosphere over the AMR with the ocean–atmosphere interaction over the North Pacific (Q. Liu et al. 2006). In the presence of the direct ENSO signal, the first MCA modes in both cases are dominated by the largely symmetric SC with lags for the winter atmosphere, reflecting

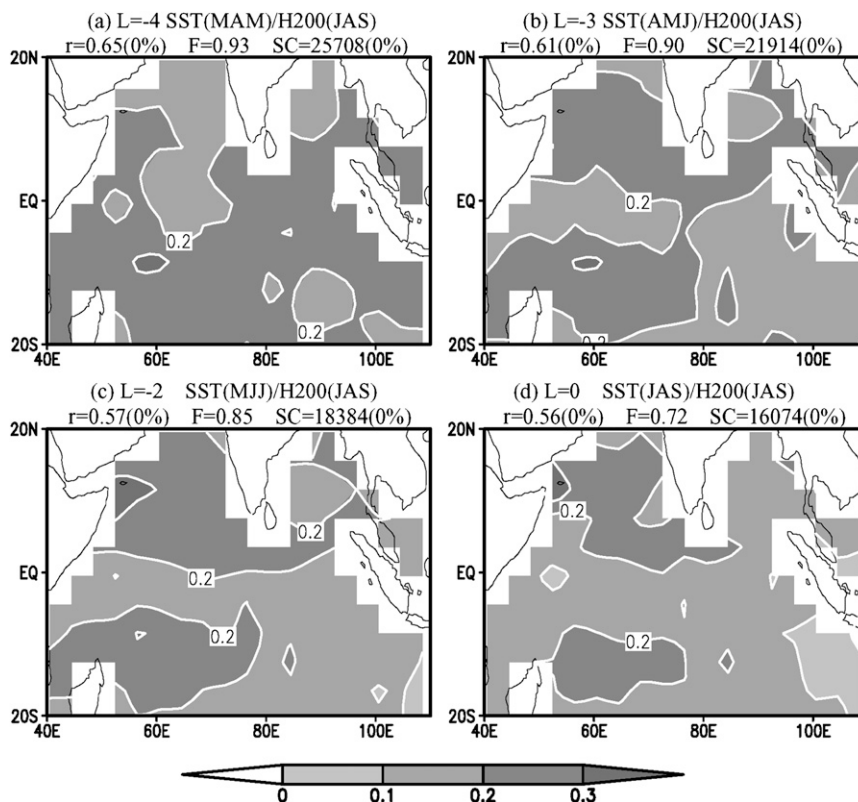


FIG. 3. Homogeneous SSTA ($^{\circ}\text{C}$) maps for the first MCA mode between the TIO SSTA and the AMR H200A without the ENSO effect. The H200A is fixed for the summer (JAS) while the SSTA leads by (a) 4, (b) 3, (c) 2, and (d) 0 months. The correlation coefficient r between the SSTA and the H200A MCA time series, the SC fraction F , and the SC of the mode are given for each lag. The percentages in parentheses for r and SC give their estimated significance levels.

the dominance of the direct ENSO influence on the winter atmosphere in both the AMR and North Pacific. After removing the direct linear ENSO signal, however, the North Pacific SC exhibits a strongly asymmetric pattern, peaking with the atmosphere leading the SSTA by about one month (Q. Liu et al. 2006), reflecting the dominant forcing of atmospheric internal variability on the North Pacific SSTA, as over the North Atlantic (Czaja and Frankignoul 2002). In the AMR, however, the dominant SC occurs with the TIO SSTA leading the AMR atmosphere by about one season. This suggests that the TIO SSTA is not affected significantly by the atmospheric variability over the AMR but plays an active role in the AMR atmosphere.

Now, we turn to the second MCA mode (Figs. 2g,h). In contrast to the first MCA mode, the second MCA mode remains similar to the mode before the removal of the direct ENSO effect signal (Figs. 2c,d). It suggests that ENSO should not significantly affect the second mode. Furthermore, the SCF of the second mode is less than 20%. The SCF of the first mode is up to 4 times that of the second mode. In addition, we want to point out

that the reduced SCF does not necessarily imply that the IOD events have less importance on the Asian monsoon. It may only reflect the smaller number of occurrences of the IOD compared to the IOB in the analysis period. Finally, the second mode tends to peak with the SCF at more than 20% for the AMR atmosphere during fall to winter, with an almost in-phase SSTA. This reflects the dominant role of the IOD in the AMR atmosphere in fall and winter, rather than in summer, and will be discussed further in section 5.

4. Possible linkage between the IOB and Asian summer monsoon

a. The SSTA pattern of the first MCA mode

Here, we further study the first MCA mode after the removal of the linear direct ENSO signal. To isolate the dominant anomalous patterns of the TIO SSTA associated with the Asian summer monsoon circulation, we plot the homogeneous SSTA (shaded) regression maps, with the H200A fixed in July–September (JAS) and the SSTA leading by 0–4 months (Figs. 3a–d). These maps

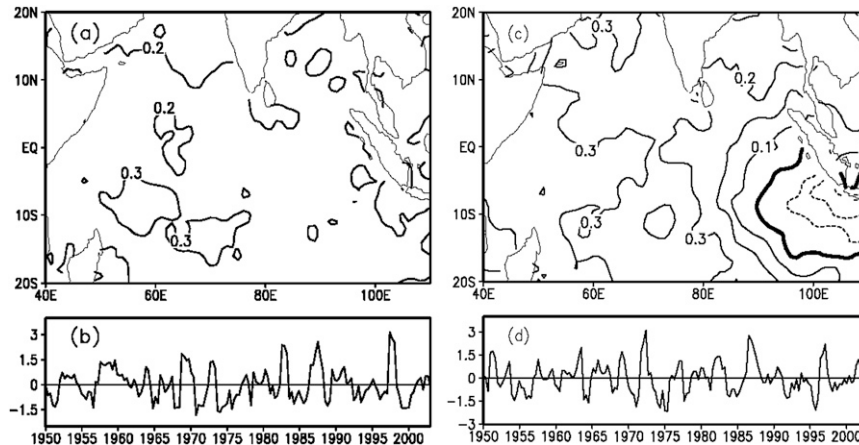


FIG. 4. The first (a) EOF and (b) time series of the spring (MAM) TIO SSTA. (c),(d) As in (a),(b), but for SSTA in autumn (SON).

represent the relatively large correlations as the SC/SCFs peaking after the removal of ENSO signal (Figs. 2e,f).

First of all, in Figs. 3a–d, the SSTA pattern exhibits a uniform basin-wide warming from spring to summer. These SSTA patterns closely resemble the IOB mode, as derived from the first EOF of the TIO SSTA in spring (Fig. 4b). It has almost perfect spatial (0.98) and temporal correlation (0.99) between the spring [March–May (MAM)] first MCA mode of SSTA (in Fig. 3a) and the first EOF mode of the SSTA (Fig. 4b). Therefore, the persisting TIO SSTA from spring to summer derived from the MCA (Figs. 3a–d) and its possible linkage to the summer atmosphere over the AMR represent the possible linkage of the IOB to the Asian summer monsoon.

Similar to the IOB, which is closely related to ENSO (e.g., Klein et al. 1999; Xie et al. 2002), the SSTA of the first MCA mode is also closely correlated to ENSO. This can be seen in Fig. 5, which shows the normalized SSTA time series obtained from the first MCA between the H200A in JAS with the ENSO signal removed and the preceding SSTA in MAM. A positive value indicates a warm SSTA over the TIO. Seven of the 10 years (1958, 1959, 1969, 1970, 1973, 1983, 1987, 1988, 1991, 1998) following the El Niño years are the warmest, except for three warm years (1959, 1969, 1991), whereas 9 of the 12 years (1951, 1956, 1965, 1968, 1974, 1975, 1976, 1984, 1985, 1989, 2000) following the La Niña years are the coolest, except for three cool years (1951, 1975, 1984). This is consistent with previous studies that showed the warm (cool) IOB events in spring are mostly induced by El Niño (La Niña) in the preceding winter (e.g., Klein et al. 1999; Xie et al. 2002).

The SSTA pattern of the IOB mode, as represented by the SSTA of the MCA first mode, persists into the summer (Figs. 3a–d). Similar persistence can also be

observed in the time series of the MCA first mode at each lag. The correlations of the time series of the MCA first mode of lag -4 (MAM) and those at lags -3 [April–June (AMJ)], -2 [May–July (MJJ)], -1 (JJA), and 0 (JAS) decrease slowly to 0.90, 0.79, 0.74, and 0.66, respectively, with all being much greater than the 95% significant level. On the mechanism of this long persistence of the IOB from spring to summer, Du et al. (2009) reveal that internal air–sea interaction within the TIO is the key to sustaining the TIO warming through summer.

b. Anomalous patterns of Asian summer monsoon

On the basis of the earlier-mentioned MCA analysis, we conclude that the dominant mode of the TIO SSTA linkage to the atmosphere over the AMR is the IOB, which can persist from spring to summer. To isolate the Asian summer monsoon anomalies' linkage to the dominant TIO, we plot the regression maps of atmospheric fields in later summer (JAS) on SSTA time series of the MCA first mode between the SSTA in MAM and subsequently AMR H200 in JAS, which represents

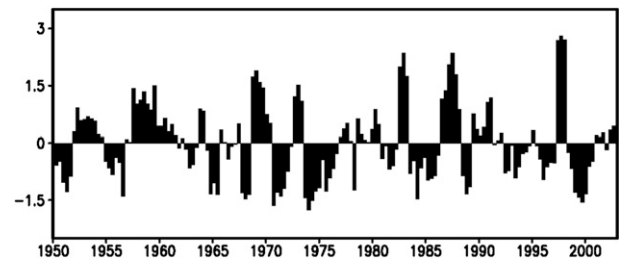


FIG. 5. Normalized SSTA time series (1950–2003) obtained from the first MCA between the H200A in JAS without the ENSO effect and the preceding SSTA in MAM, e.g., the latter leading the former by 4 months. Each year consists of three vertical bars (MAM). When it is positive, it indicates a warm SSTA of the TIO.

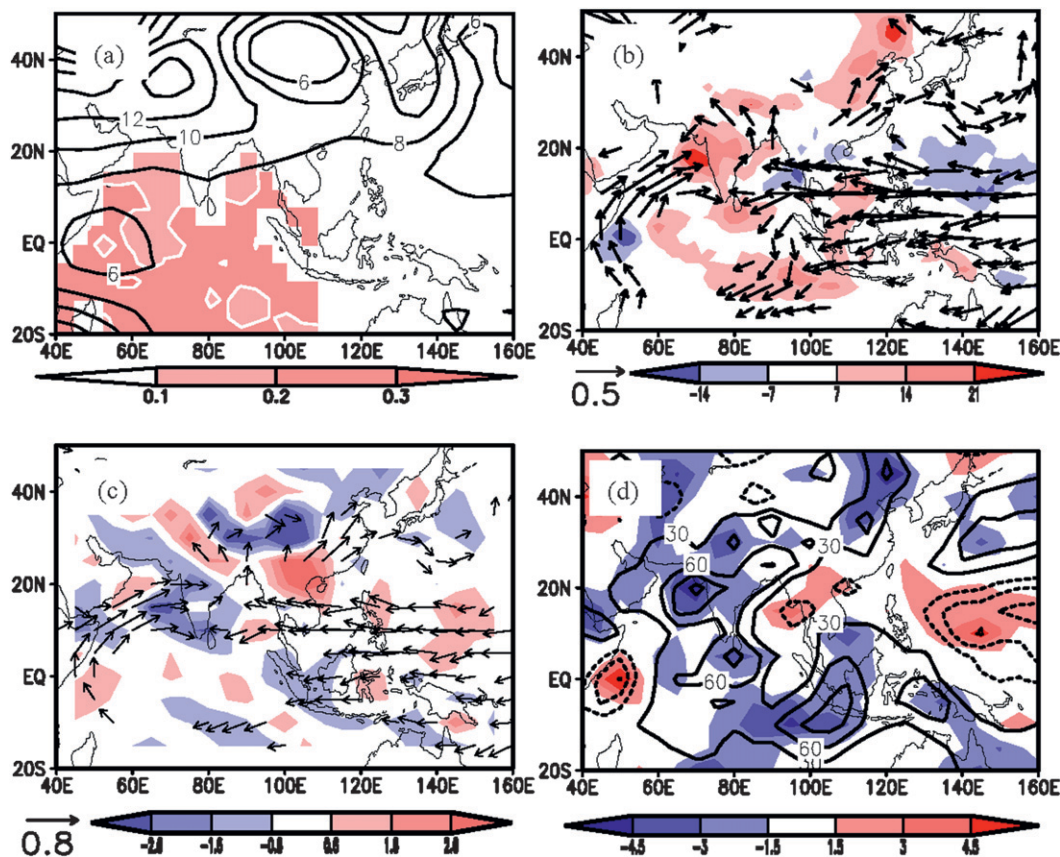


FIG. 6. Regression maps of the (a) H200A (contour, m) in JAS and SST in MAM (colors, $^{\circ}\text{C}$), (b) wind at 850 hPa (vector, m s^{-1}) and precipitation rate (colors, mm month^{-1}) in JAS, (c) transport of specific humidity at 850 hPa (vector, $10^{-1} \text{ kg s}^{-1} \text{ hPa}^{-1} \text{ m}^{-1}$) and its divergence (colors, $10^{-6} \text{ kg s}^{-1} \text{ hPa}^{-1} \text{ m}^{-2}$) in JAS, and (d) vertically integrated heat source (contour, W m^{-2}) and vertical velocity at 500 hPa (colors, $10^{-3} \text{ Pa s}^{-1}$) in JAS on the SSTA time series of the first MCA mode. Only anomalies significant at the 95% confidence level are shown.

the peak SC-SCF after removing the ENSO signal (Figs. 2e,f). These regression atmospheric fields include the H200A (Fig. 6a), precipitation and horizontal wind at 850 hPa (Fig. 6b), moisture transport and its divergence at 850 hPa (Fig. 6c), and column-integrated diabatic heating and atmosphere vertical velocity at 500 hPa (Fig. 6d).

At the upper level, associated with a warm IOB, the H200A in JAS is characterized by two anomalous highs locating over the western portion of the Tibetan Plateau and the Japan Sea (Fig. 6a). The first high is likely a Rossby wave response—that is, a likely type of the “Matsuno–Gill pattern”—to a diabatic heating over the South Asia and the TIO. This high center may contribute to enhancing the South Asian high. Also, there appears to be a large-scale high-anomaly region over the AMR, which is associated with the warm TIO SST (Meehl et al. 2003), with the second high center over the Japan Sea. The second high is associated with the Bonin high and helps to bring hot summer air to Japan (Enomoto

et al. 2003). This high is proposed to be a result of the propagation of stationary Rossby wave energy along the East Asian jet stream from the first high anomaly through a circuglobe teleconnection in the midlatitude atmosphere in boreal summer (Ding and Wang 2005). This issue is studied in detail in Yang et al. (2009).

Significant anomalies of atmospheric circulation associated with the IOB can also be found at the lower level. A warm IOB SSTA is a linkage to an easterly anomaly that spans from the western Pacific to the eastern TIO (Fig. 6b) and a subsequent moisture transport from the western Pacific into the eastern TIO (Fig. 6c). This anomalous easterly transport leads to a moisture divergence (Fig. 6c) and to reduced precipitation (Fig. 6b) in the western Pacific, and to a moisture convergence (Fig. 6c) and increased precipitation (Fig. 6b) around the central-eastern TIO. This anomalous easterly can also be reinforced by an enhanced diabatic heating associated with an upward velocity and latent heat release around the central-eastern TIO, and a downward

velocity and reduced diabatic heating in the western Pacific (Fig. 6d).

In the meantime, a surface anticyclone anomaly is generated over the northwestern tropical Pacific and the South China Sea with increased surface southerly (Fig. 6b) and in turn moisture transport into East Asia (Fig. 6c). This leads to an anomalous moisture convergence (Fig. 6c), an ascending air and latent heat release (Fig. 6d), and precipitation (Fig. 6b) over East Asia, but an anomalous moisture divergence (Fig. 6c), a descending air and reduced latent heat release (Fig. 6d), and reduced precipitation (Fig. 6b) over the western Philippines. An earlier study by Chang et al. (2000) has shown that the strength, location, and spatial extent of the Pacific subtropical high are related to the Indian Ocean SSTA. The rainfall distribution over East Asia also depends on the location of this subtropical high. The earlier-mentioned atmospheric anomalies at the lower level in JAS are consistent with the model simulations in spring of Annamalai et al. (2005a,b), which shows a warm IOB in spring inducing atmosphere Kelvin wave in the western Pacific with anomalous easterlies and an anticyclonic circulation anomaly. The associated changes in the Indian Ocean Walker circulation suppress precipitation over the tropical western Pacific–Maritime Continent and contribute to the development of a lower-level anticyclone over the Philippines. Their model results further indicate that more than half of the total precipitation anomalies over the tropical western Pacific–Maritime Continent are forced by remote TIO SSTA. This offers an additional mechanism for the generation of the Philippine Sea anticyclone, in addition to the Pacific SSTA forcing.

Another significant anomaly at the lower level is more monsoon precipitation around South Asia, that is, the eastern Arabian Sea and India, accompanied by a stronger anomalous southwesterly from the equatorial western Indian Ocean to the eastern Arabian Sea, that is, a stronger Somali jet and Indian summer monsoon (Fig. 6b). Similar results appear too in late summer (August–September), those associated with a warm northern Indian Ocean SST in a recent study based on an observational analysis and numerical experiment (Park et al. 2009). While these anomalies in summer are different from those in spring (Annamalai et al. 2005a,b). We propose this difference comes from the onset of the climatological South Asian summer monsoon. In summer after the onset of the southwesterly summer monsoon wind, the southwesterly wind of the summer monsoon can transport more moisture (Fig. 6c) associated with the warm IOB into South Asia (X. Liu et al. 2006) and in turn induce an upward vertical velocity anomaly center (Fig. 6d) and more precipitation (Fig. 6b) over South Asia.

This increased precipitation around South Asia forms a new atmospheric heating source over the northeastern Arabian Sea, which is associated with the warm IOB and is responsible for the positive height anomaly west to the Tibetan Plateau at the upper level, as suggested earlier (Fig. 6d). In addition, a small negative precipitation center can be seen over the Somali coast. This anomaly may be associated with a small negative SSTA center over the Somali coast, which can be induced by a stronger Somali jet stream through upwelling.

The atmospheric anomalies associated with the IOB presented in this article are consistent with our previous investigation using correlation analysis and numerical experiments (J. Yang et al. 2007). We can therefore conclude that using another unique method—the MCA—the results of atmospheric anomalies associated the IOB are now confirmed.

c. Composite analysis

The earlier-mentioned conclusion obtained from the MCA and regression analysis is further supported by a composite analysis. Following J. Yang et al. (2007), a total of 11 warm (1958, 1959, 1969, 1970, 1973, 1983, 1987, 1988, 1991, 1998, 2003) and 11 cold (1955, 1956, 1965, 1968, 1971, 1974, 1984, 1985, 1989, 1994, 2000) years are chosen when the April IOB index exceeds 0.75 and -0.75 standard deviation, respectively. The IOB index is defined as the time series of the first EOF mode of the SSTA over the TIO. The 11 warm and 11 cold IOB events form a composite (warm events minus cold events) for the SSTA and atmospheric circulation in summer (JAS). These composite maps of the H200A and the SSTA (Fig. 7a), 850-hPa wind, and precipitation rate (Fig. 7b) agree well with the corresponding regression maps of the MCA (Figs. 6a,b).

Furthermore, if we make a composite of the anomalies for the years that follow ENSO but without the typical IOB (4 warm years: 1966, 1977, 1992, 1995; one cool year: 2001) as in Figs. 7c,d, then most features of the SSTA and the H200A and the lower-level circulation in the TIO associated with the IOB disappear. Only the increased precipitation over the eastern Arabian Sea has some similarity between the years with the IOB in Fig. 7b and those without the IOB in Fig. 7d; however, this anomalous precipitation in Fig. 7d without the IOB may be only associated with the local warm SST of the Arabian Sea. This is because the anomalous stronger southwesterly wind and stronger Somali jet stream, which are associated with the IOB in Fig. 7b, are not found in Fig. 7d. At the same time, we notice that the anomalous anticyclones over the northwest Pacific in Fig. 7d are similar with those in Fig. 7b. These anomalous anticyclones can be induced by the local SSTA due to ENSO,

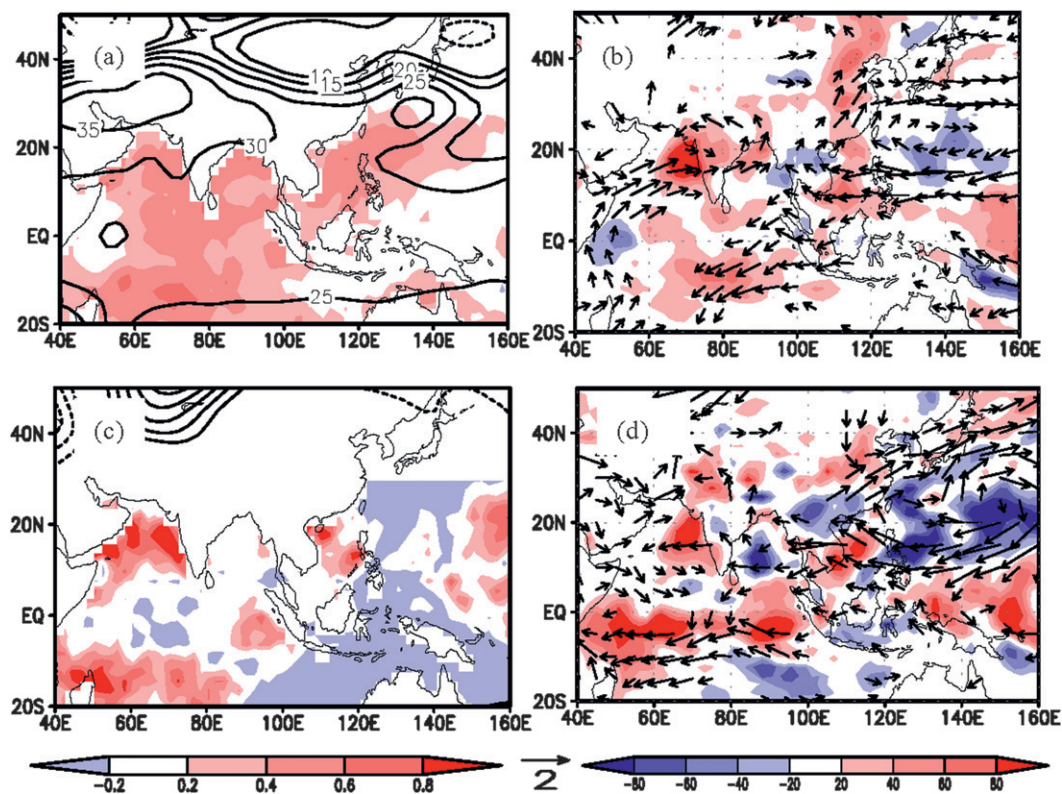


FIG. 7. Differences of the composite maps in JAS between warm and cold IOB years: (a) H200A (contour, m) and SSTA (colors, $^{\circ}\text{C}$) and (b) winds at 850 hPa (vector, m s^{-1}) and precipitation rate (shading, mm month^{-1}). (c), (d) As in (a), (b), respectively, but for the years of decaying ENSO without the IOB. Only anomalies significant at the 95% confidence level are shown.

as noted by previous studies (e.g., Lau and Nath 2003; Wang et al. 2003; Lau et al. 2004; Lau and Wang 2005). However, as we proposed in J. Yang et al. (2007), the IOB can also contribute to form the anomalous anticyclone over the northwest Pacific Ocean.

On the other hand, it is well known that the precipitation pattern associated with ENSO is dominated by negative rainfall anomalies over the western Pacific, Maritime Continent, the equatorial eastern Indian Ocean, and the southern Bay of Bengal, while positive centers are located over the northern Bay of Bengal, southern China, and the western Indian Ocean. The main feature of low-level circulation is a broad region of divergent flow emanating from the Maritime Continent, with westerlies spanning the entire tropical Pacific and easterlies over the TIO. This further substantiates our conclusion that the atmosphere anomaly over the AMR associated with the IOB is not directly linked to the tropical Pacific SSTA but to the TIO SSTA. Therefore, the TIO acts as a “capacitor” with the ENSO charging the TIO IOB, which after the linear-direct ENSO SSTAs vanish, recharges the anomaly signal and feeds it back to the atmosphere over the AMR. In summer, this IOB role is

enhanced significantly by the northward water vapor transport and additional heating source formation.

5. Monsoon anomalies associated with the IOD

The IOD effect on the atmosphere anomaly in the AMR is very different from the IOB effect; because the IOD peak appears in fall, the maximum of atmosphere response should be in fall or winter.

a. Winter monsoon and IOD

Now, we discuss the second MCA mode after removing the linear direct ENSO signal. From the MCA results in Figs. 2g,h, it is clear that the AMR atmosphere in early winter [November–January (NDJ)] has a maximum significant (i.e., corresponding to the largest SC–SCF) relationship with the TIO SSTA in late fall (OND), as the latter leads the former by about one month. Figure 8a shows the regression maps of the SSTA in OND and the H200A in NDJ. The SSTA pattern is characterized by a negative SSTA in the eastern TIO and positive SSTA in the western TIO. This pattern resembles the IOD mode (Saji et al. 1999; Webster et al.

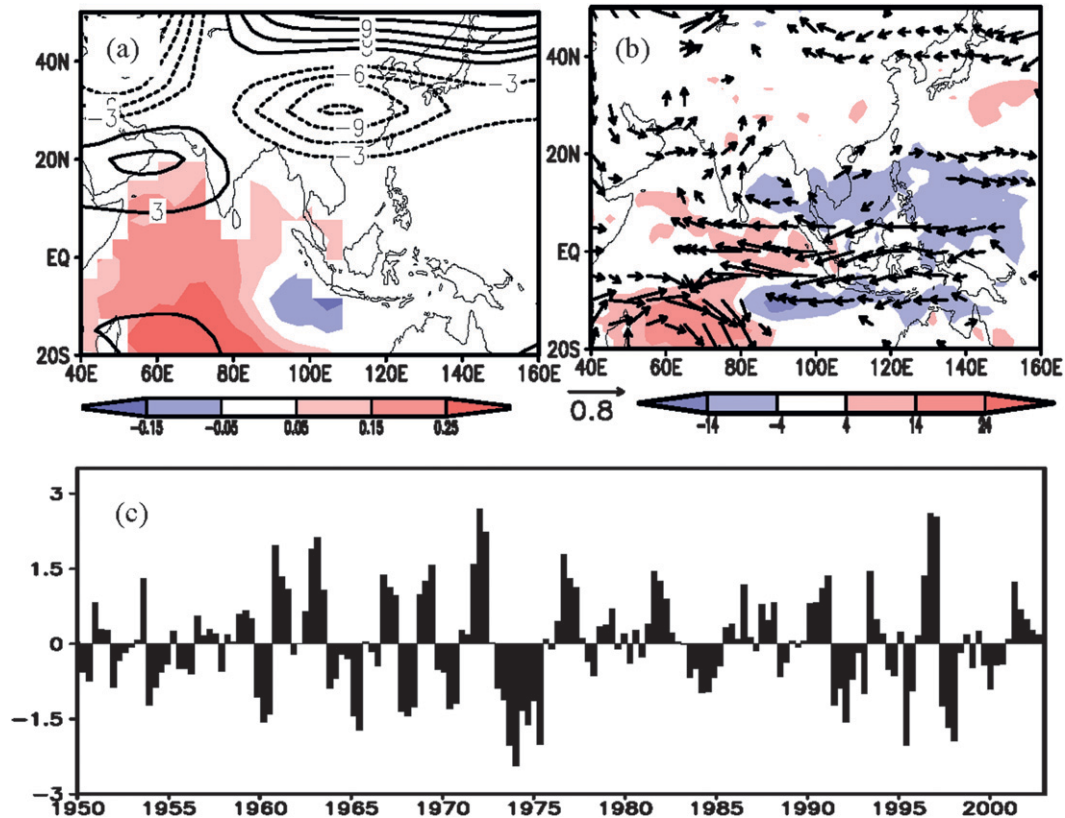


FIG. 8. Regression maps for (a) H200A (contour, m) in NDJ and SSTA (colors, °C) in OND and (b) horizontal wind at 850 hPa (vector, m s^{-1}) and precipitation rate (colors, mm month^{-1}) in NDJ. The regression maps are on the SSTA time series of the second MCA mode between H200A in NDJ without the ENSO effect and the preceding SSTA in OND (e.g., the latter leading the former by 1 month). (c) The time series. Only anomalies significant at the (a) 95% and (b) 90% confidence levels are shown.

1999) very well. The pattern correlation with the first EOF mode of the TIO SSTA in fall (Fig. 4c) is 0.90, and the corresponding time series of the second MCA mode (Fig. 8c) and the first EOF SSTA mode in fall also correlates highly at 0.79. Therefore, in the fall, the second MCA mode of the TIO SSTA captures mostly features usually called the IOD mode (Saji et al. 1999; Webster et al. 1999).

It should be noted that late fall is the time of strongest IOD linking to the atmosphere anomaly over the AMR, because the IOD peaks in late fall. Yet, in this period the Asian summer monsoon has ceased, while the Asian winter monsoon is being established. This implies that the strongest linkage of the IOD to the atmosphere anomaly over the AMR occurs after fall. Associated with the IOD in fall, the H200A in winter exhibits negative anomaly around East Asia and eastern Europe, and positive anomaly over areas west to India at the upper level (Fig. 8a). At the lower level, we can see that an anomalous easterly is over the eastern TIO–western Pacific, southwesterly anomalies over South Asia, and a cyclonic circulation in the southwestern TIO (Fig. 8b). Correspondingly,

more precipitation is over the southwestern TIO and eastern equatorial Indian Ocean and less precipitation over the southeastern TIO, South China Sea, and northwestern subtropical Pacific.

It is safe to say that a positive-phase IOD SSTA (negative SSTA in the eastern TIO) tends to decrease the South Asian winter monsoon over the TIO and has a possibility of inducing the above-mentioned atmosphere circulation and precipitation anomalies in winter. Here, the new finding is the role of the IOD in the Asian winter monsoon. Although the probable mechanism of the IOD linkage to the winter monsoon is not central to the current study, it is important to recognize this relationship, which will be studied further in the near future.

b. Summer monsoon and IOD

In the mean time, the MCA results (Figs. 2g,h) also show the IOD correlates to the Asian summer monsoon. However, this relationship between the IOD in JAS and the summer atmosphere anomaly is significant only at the 90% level, not at the 99% level, and accounts for less

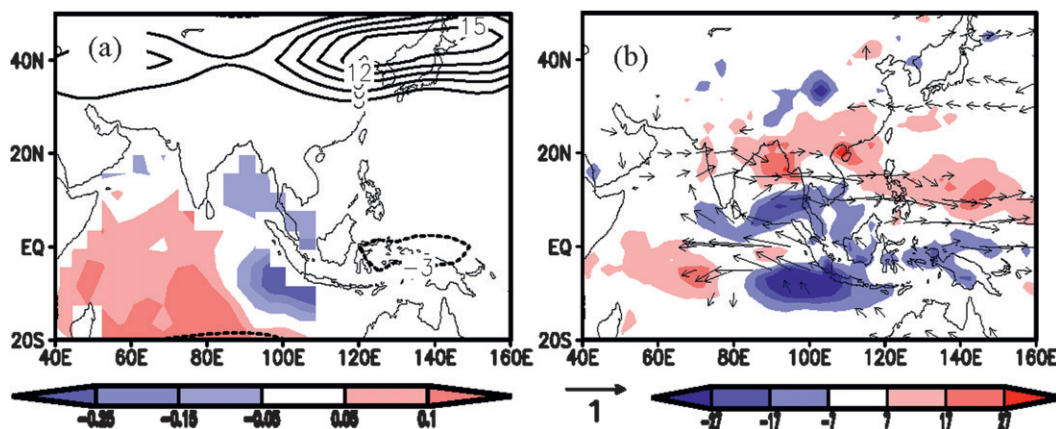


FIG. 9. (a),(b) As in Figs. 8a,b, respectively, but for the MCA between the H200A and the SSTA; both at JAS (lag 0). Only anomalies significant at the 95% confidence level are shown.

than 10% of the total SC. This is much smaller than the IOB correlation to the Asian summer monsoon, which amounts to more than 90% in the SCF (Fig. 2f).

In summer (JAS), associated with the IOD SSTA (Fig. 9a), there appears a surface easterly across the eastern-central TIO that enhances the southerly surface wind over the northern TIO, and in turn the convergence of moisture and eventually precipitation over the southwestern Indian Ocean, the northern Bay of Bengal, the northern South China Sea, and south China (Fig. 9b).

We notice these atmospheric anomalous patterns (Fig. 9) are consistent with previous results about the IOD effect on atmosphere in summer (e.g., Chang et al. 2000; Li et al. 2001; Guan et al. 2003; Saji and Yamagata 2003). These studies suggested that the IOD can induce the Indian summer monsoon (ISM) to be stronger. We should point out that it is difficult to identify the cause and effect based on only the covariability patterns of the earlier-mentioned analysis, since these (Fig. 9) are simultaneous and not the IOD leading the atmosphere. In fact, the relationship between the IOD events and the ISM is a controversial issue. One suggestion is that positive IOD events enhance ISM rainfall (i.e., Ashok et al. 2001; Li et al. 2003), although Li et al. (2003) argued that the strong ISM will tend to damp the original IOD event. Others suggested that positive IOD events normally coincide with dry conditions over the Indian subcontinent (Webster et al. 2002; Loschnigg et al. 2003; Meehl et al. 2003; Terray et al. 2005); therefore, this issue needs further study.

6. Conclusions and discussions

In this study, we systematically analyze the possible linkage between the TIO SSTA and the atmosphere circulation over the AMR in the observation using the MCA. After removing the linear ENSO effect from the

atmospheric data, the two leading MCA modes of the TIO SSTA and the atmosphere are found, and they correspond to the IOB and IOD, respectively. The IOB is found to be the dominant SSTA mode that links with the summer monsoon, with a SC of up to 90%.

Consistent with the correlation analysis and numerical experiments of J. Yang et al. (2007), our MCA analysis suggests that the IOB acts as a delayed relay of the ENSO signal from the tropical Pacific to the Asian summer monsoon. A warm TIO persisting from spring to summer tends to enhance the summer monsoon significantly through the enhanced moisture transport, enhancing summer monsoon precipitation after the establishment of the climatological summer monsoon wind. The IOB role in the Asian monsoon is enlarged by the climatological summer monsoon.

In comparison, the IOD is most effective in correlating with the Asian winter monsoon establishment in late fall, with a positive IOD leading a weaker winter monsoon. The IOD linkage to the Asian monsoon in general, however, is weak, accounting for less than 20% of the total SC. Therefore, more studies on the IOB linkage to the monsoon, especially the mechanism, are needed in the future.

Acknowledgments. We would like to acknowledge the discussions with Drs. Shang-Ping Xie, Lixin Wu, and Yunlai Zhu and programming assistance from Dr. Na Wen. This research is supported by the Chinese NSF Grant 40830106, the 111 Project under Grant B07036, and the Chinese Grant the Public Sector (Meteorology) Research and Special Project GYHY200906016.

REFERENCES

Alexander, M. A., N.-C. Lau, and J. D. Scott, 2004: Broadening the atmospheric bridge paradigm: ENSO teleconnections to the

- tropical west Pacific-Indian Oceans over the seasonal cycle and to the North Pacific in summer. *Earth's Climate: The Ocean-Atmosphere Interaction: From Basin to Global Scales, Geophys. Monogr.*, Vol. 147, Amer. Geophys. Union, 85–103.
- Annamalai, H., P. Liu, and S.-P. Xie, 2005a: Southwest Indian Ocean SST variability: Its local effect and remote influence on Asian monsoons. *J. Climate*, **18**, 4150–4167.
- , S.-P. Xie, J. P. McCreary, and R. Murtugudde, 2005b: Impact of Indian Ocean sea surface temperature on developing El Niño. *J. Climate*, **18**, 302–319.
- Ashok, K., Z. Guan, and T. Yamagata, 2001: Impact of the Indian Ocean dipole on the relationship between the Indian monsoon rainfall and ENSO. *Geophys. Res. Lett.*, **28**, 4499–4502.
- Behera, S. K., and T. Yamagata, 2003: Influence of the Indian Ocean Dipole on the Southern Oscillation. *J. Meteor. Soc. Japan*, **81**, 169–177.
- , R. Krishnan, and T. Yamagata, 1999: Unusual ocean-atmosphere conditions in the tropical Indian Ocean during 1994. *Geophys. Res. Lett.*, **26**, 3001–3004.
- Bretherton, C. S., C. S. Smith, and J. M. Wallace, 1992: An intercomparison of methods for finding coupled patterns in climate data. *J. Climate*, **5**, 541–560.
- Chang, C. P., Y. Zhang, and T. Li, 2000: Interannual and interdecadal variations of the East Asian summer monsoon and tropical Pacific SSTs. Part II: Meridional structure of the monsoon. *J. Climate*, **13**, 4326–4340.
- Chiang, J. C. H., and A. H. Sobel, 2002: Tropical tropospheric temperature variations caused by ENSO and their influence on the remote tropical climate. *J. Climate*, **15**, 2616–2631.
- Clark, C. O., J. E. Cole, and P. J. Webster, 2000: Indian Ocean SST and Indian summer rainfall: Predictive relationships and their decadal variability. *J. Climate*, **13**, 2503–2519.
- Czaja, A., and C. Frankignoul, 2002: Observed impact of Atlantic SST anomalies on the North Atlantic Oscillation. *J. Climate*, **15**, 606–623.
- Ding, Q., and B. Wang, 2005: Circumglobal teleconnection in the Northern Hemisphere summer. *J. Climate*, **18**, 3483–3505.
- Du, Y., S.-P. Xie, G. Huang, and K. Hu, 2009: Role of air–sea interaction in the long persistence of El Niño-induced North Indian Ocean warming. *J. Climate*, **22**, 2023–2038.
- Enomoto, T., B. J. Hoskins, and Y. Matsuda, 2003: The formation mechanism of the Bonin high in August. *Quart. J. Roy. Meteor. Soc.*, **129**, 157–178.
- Frankignoul, C., and N. Sennechael, 2007: Observed influence of North Pacific SST anomalies on the atmospheric circulation. *J. Climate*, **20**, 592–606.
- Gill, A. E., 1980: Some simple solutions for heat-induced tropical circulation. *Quart. J. Roy. Meteor. Soc.*, **106**, 447–462.
- Guan, Z., K. Ashok, and T. Yamagata, 2003: Summer-time response of the tropical atmosphere to the Indian Ocean dipole sea surface temperature anomalies. *J. Meteor. Soc. Japan*, **81**, 531–561.
- Izumo, T., C. B. Montégut, J.-J. Luo, S. K. Behera, S. Masson, and T. Yamagata, 2008: The role of the western Arabian Sea upwelling in Indian monsoon rainfall variability. *J. Climate*, **21**, 5603–5623.
- Kalnay, E., and Coauthors, 1996: The NCEP/NCAR 40-Year Reanalysis Project. *Bull. Amer. Meteor. Soc.*, **77**, 437–471.
- Klein, S. A., B. J. Sode, and N.-C. Lau, 1999: Remote sea surface temperature variations during ENSO: Evidence for a tropical atmospheric bridge. *J. Climate*, **12**, 917–932.
- Kripalani, R. H., and P. Kumar, 2004: Northeast monsoon rainfall variability over south peninsular India vis-à-vis the Indian Ocean Dipole mode. *Int. J. Climatol.*, **24**, 1267–1282.
- , J. H. Oh, J. H. Kang, S. S. Sabade, and A. Kulkarni, 2005: Extreme monsoons over East Asia: Possible role of the Indian Ocean Zonal Mode. *Theor. Appl. Climatol.*, **82**, 81–94.
- Kulkarni, A., S. S. Sabade, and R. H. Kripalani, 2007: Association between extreme monsoons and the dipole mode over the Indian subcontinent. *Meteor. Atmos. Phys.*, **95**, 255–268.
- Kumar, A., and M. Hoerling, 2003: The nature and causes for the delayed atmospheric response to El Niño. *J. Climate*, **16**, 1391–1403.
- Lareef, Z., S. A. Rao, and T. Yamagata, 2003: Modulation of Sri Lanka *Maha* rainfall by the Indian Ocean Dipole. *Geophys. Res. Lett.*, **30**, 1063, doi:10.1029/2002GL015639.
- Lau, N.-C., and M. J. Nath, 2000: Impact of ENSO on the variability of the Asian–Australian monsoons as simulated in GCM experiments. *J. Climate*, **13**, 4287–4309.
- , and —, 2003: Atmosphere–ocean variations in the Indo-Pacific sector during ENSO episodes. *J. Climate*, **16**, 3–20.
- , and —, 2004: Coupled GCM simulation of atmosphere–ocean variability associated with zonally asymmetric SST changes in the tropical Indian Ocean. *J. Climate*, **17**, 245–265.
- , and B. Wang, 2005: Interactions between the Asian monsoon and the El Niño/Southern Oscillation. *The Asian Monsoon*, B. Wang, Ed., Springer Praxis Publishing, 479–511.
- , M. J. Nath, and H. Wang, 2004: Simulations by a GFDL GCM of ENSO-related variability of the coupled atmosphere–ocean system in the East Asian monsoon region. *East Asian Monsoon*, C. P. Chang, Ed., World Scientific Series on Asia-Pacific Weather and Climate, Vol. 2, World Scientific, 271–300.
- , A. Leetmaa, M. J. Nath, and H.-L. Wang, 2005: Influences of ENSO-induced Indo–western Pacific SST anomalies on extratropical atmospheric variability during the boreal summer. *J. Climate*, **18**, 2922–2942.
- Li, C., and M. Mu, 2001: The influence of the Indian Ocean dipole on atmospheric circulation and climate. *Adv. Atmos. Sci.*, **18**, 831–843.
- Li, S. L., J. Lu, G. Huang, and K. Hu, 2008: Tropical Indian Ocean basin warming and East Asian summer monsoon: A multiple AGCM study. *J. Climate*, **21**, 6080–6088.
- Li, T., Y. Zhang, C.-P. Chang, and B. Wang, 2001: On the relationship between Indian Ocean sea surface temperature and Asian summer monsoon. *Geophys. Res. Lett.*, **28**, 2843–2846.
- , B. Wang, C.-P. Chang, and Y. Zhang, 2003: A theory for the Indian Ocean dipole–zonal mode. *J. Atmos. Sci.*, **60**, 2119–2135.
- Liu, Q., N. Wen, and Z. Liu, 2006: An observational study of the impact of the North Pacific SST on the atmosphere. *Geophys. Res. Lett.*, **33**, L18611, doi:10.1029/2006GL026082.
- Liu, X., Z. Liu, J. E. Kutzbach, S. C. Clements, and W. L. Prell, 2006: Hemispheric insolation forcing of the Indian Ocean and Asian monsoon: Local versus remote impacts. *J. Climate*, **19**, 6195–6208.
- Loschnigg, J., G. A. Meehl, J. M. Arblaster, G. P. Compo, and P. J. Webster, 2003: The Asian monsoon, the tropospheric biennial oscillation, and the Indian Ocean dipole in the NCAR CSM. *J. Climate*, **16**, 1617–1642.
- Meehl, G. A., 1997: The South Asian monsoon and the tropospheric biennial oscillation. *J. Climate*, **10**, 1921–1943.
- , and J. M. Arblaster, 2002: Indian monsoon GCM sensitivity experiments testing tropospheric biennial oscillation transition conditions. *J. Climate*, **15**, 923–944.
- , —, and J. Loschnigg, 2003: Coupled ocean–atmosphere dynamical processes in the tropical Indian and Pacific Oceans and the TBO. *J. Climate*, **16**, 2138–2158.

- Park, H.-S., J. C. H. Chiang, B. R. Lintner, and G. J. Zhang, 2009: The delayed effect of major El Niño events on Indian monsoon rainfall. *J. Climate*, **23**, 932–946.
- Park, S., M. A. Alexander, and C. Deser, 2006: The impact of cloud radiative feedback, remote ENSO forcing, and entrainment on the persistence of North Pacific sea surface temperature anomalies. *J. Climate*, **19**, 6243–6261.
- Saji, N. H., and T. Yamagata, 2003: Possible impacts of Indian Ocean Dipole mode events on global climate. *Climate Res.*, **25**, 151–169.
- , B. N. Goswami, P. N. Vinayachandran, and T. Yamagata, 1999: A dipole mode in the tropical Indian Ocean. *Nature*, **401**, 360–363.
- Shinoda, T., M. A. Alexander, and H. H. Hendon, 2004: Remote response of the Indian Ocean to interannual SST variations in the tropical Pacific. *J. Climate*, **17**, 362–372.
- Slingo, J. M., and H. Annamalai, 2000: The El Niño of the century and the response of the Indian summer monsoon. *Mon. Wea. Rev.*, **128**, 1778–1797.
- Terray, P., S. Dominiak, and P. Delecluse, 2005: Role of the southern Indian Ocean in the transitions of the monsoon–ENSO system during recent decades. *Climate Dyn.*, **24**, 169–195.
- Wang, B., R. G. Wu, and X. Fu, 2000: Pacific East Asian teleconnections: How does ENSO affect East Asian climate? *J. Climate*, **13**, 1517–1536.
- , R. Wu, and T. Li, 2003: Atmosphere–warm ocean interaction and its impacts on Asian–Australian monsoon variation. *J. Climate*, **15**, 1195–1211.
- Watanabe, M., and F.-F. Jin, 2003: A moist linear baroclinic model: Coupled dynamical–convective response to El Niño. *J. Climate*, **16**, 1121–1139.
- Webster, P. J., A. M. Moore, J. P. Loschnigg, and R. R. Leben, 1999: Coupled ocean–atmosphere dynamics in the Indian Ocean during 1997–98. *Nature*, **401**, 356–360.
- , C. Clark, G. Cherikova, J. Fasullo, W. Han, J. Loschnigg, and K. Sahami, 2002: The monsoon as a self-regulating coupled ocean–atmosphere system. *Meteorology at the Millennium*, R. P. Pearce, Ed., International Geophysics Series, Vol. 83, Academic Press, 198–219.
- Wu, R., B. P. Kirtman, and V. Krishnamurthy, 2008: An asymmetric mode of tropical Indian Ocean rainfall variability in boreal spring. *J. Geophys. Res.*, **113**, D05104, doi:10.1029/2007JD009316.
- Xie, S.-P., H. Annamalai, F. A. Schott, and J. P. McCreary, 2002: Structure and mechanisms of south Indian Ocean climate variability. *J. Climate*, **15**, 864–878.
- , K. Hu, G. Huang, J. Hafner, H. Tokinaga, T. Sampe, and Y. Du, 2009: Indian Ocean capacitor effect on Indo–western Pacific climate during the summer following El Niño. *J. Climate*, **22**, 730–747.
- Yanai, M., and T. Tomita, 1998: Seasonal and interannual variability of atmospheric heat sources and moisture sinks as determined from NCEP–NCAR reanalysis. *J. Climate*, **11**, 463–482.
- Yang, J., Q. Liu, S.-P. Xie, Z. Liu, and L. Wu, 2007: Impact of the Indian Ocean SST basin mode on the Asian summer monsoon. *Geophys. Res. Lett.*, **34**, L02708, doi:10.1029/2006GL028571.
- , —, Z. Liu, L. Wu, and F. Huang, 2009: Basin mode of Indian Ocean sea surface temperature and Northern Hemisphere circumglobal teleconnection. *Geophys. Res. Lett.*, **36**, L19705, doi:10.1029/2009GL039559.
- Yang, S., X. Ding, D. Zhang, and S.-H. Yoo, 2007: Time-frequency characteristics of the relationships between tropical Indo-Pacific SSTs. *Adv. Atmos. Sci.*, **24**, 343–359.
- Yoo, S.-H., S. Yang, and C.-H. Ho, 2006: Variability of the Indian Ocean sea surface temperature and its impacts on Asian–Australian monsoon climate. *J. Geophys. Res.*, **111**, D03108, doi:10.1029/2005JD006001.
- Yuan, Y., H. Yang, W. Zhou, and C. Li, 2008a: Influences of the Indian Ocean Dipole on the Asian summer monsoon in the following year. *Int. J. Climatol.*, **28**, 1849–1859.
- , W. Zhou, J. Chan, and C. Li, 2008b: Impacts of the basin-wide Indian Ocean SSTA on the South China Sea summer monsoon onset. *Int. J. Climatol.*, **28**, 1579–1587.
- Zhu, Y. L., 1993: The large-scale hydrological cycle and its role in Asian summer monsoon variations induced by Indian Ocean sea surface temperature anomalies. Ph.D thesis, University of Wisconsin—Madison, 205 pp.
- , and D. D. Houghton, 1996: The impact of Indian Ocean SST on the large-scale Asian summer monsoon and the hydrological cycle. *Int. J. Climatol.*, **16**, 617–632.